ADVANCED FUNCTIONAL MATERIALS

Supporting Information

for *Adv. Funct. Mater.*, DOI: 10.1002/adfm. 201200676

Visualizing Strain Evolution and Coordinated Buckling within CNT Arrays by In Situ Digital Image Correlation

*Matthew R. Maschmann , Gregory J. Ehlert , Sei Jin Park , David Mollenhauer , Benji Maruyama , A. John Hart , and Jeffery W. Baur **

Submitted to ADVANCED FUNCTIONAL MATERIALS

Supporting Information:

Advanced Functional Materials, "Visualizing Strain Evolution and Coordinated Buckling within CNT Arrays by *in situ* Digital Image Correlation," by Matthew R. Maschmann, Gregory J. Ehlert, Sei Jin Park, David Mollenhauer, Benji Maruyama, A. John Hart, and Jeffery W. Baur

S1. SEM Imaging Conditions

Imaging conditions were selected such that the resulting pixel dimensions were similar to the diameters of the individual CNTs within the CNT array columns. Typical magnifications for DIC analysis ranged from approximately 3,000 – 9,000x, with typical image resolutions ranging from 1,500 x 2,000 – 3,000 x 3,000 pixels. The resulting pixel size ranged from approximately 10 – 40 nm. Typical SEM micrographs utilized for DIC analysis are displayed in **Figure S1**. These micrographs are obtained from the imaging of a 30 μm wide, 25 μm tall and a 30 μm wide, 75 μm tall CNT columns. Each image includes an inset that is enlarged by a factor of 10 to illustrate the typical CNT array feature size relative to the pixel dimensions. The images clearly demonstrate that individual CNTs and CNT bundles may be distinguished and utilized by DIC to track the relative motion under compressive loading.

S2. SEM Image Drift and Distortion

Imaging artifacts arising from SEM drift and rastering inconsistencies are potential sources of error for DIC analysis of *in situ* testing. To quantify their impact relative to the *in situ* SEM compression of CNT array columns, a 30 μm wide, 75 μm tall CNT column was subjected to the typical imaging conditions utilized during mechanical testing. The image resolution was 1500 x 2000 pixels, with a dwell time of 10 μs per pixel. A series of 100 micrographs were obtained over a duration of approximately 2.5 hours. The sequence of micrographs was examined by DIC, with analysis of the final micrograph displayed in Figure S2.

Image drift in the vertical direction, parallel to the axis of the CNT array column, was small and relatively uniform over the length of the column, as observed in Figure S2a. The magnitude of the drift ranged from 5.77 – 6.53 pixels, resulting in a vertical distortion of 0.76 pixels. The minor principal strain resulting from the image distortions was also small, ranging from -0.2% – 0.1% (Figure S2b). These values are small relative to the mechanical deformation imposed during compression and are randomly distributed throughout the column during the 2.5 hour analysis window. The magnitude and distribution of the SEM imaging artifacts are sufficiently small and random that their contribution to the observed trends with respect to CNT array column deformation is negligible.

S3. DIC Output Example

The metrics of vertical displacement (V), horizontal displacement (U), horizontal strain (ε_{xx}), and shear strain (ε_{xy}), were examined for each column, in addition to the quantities vertical strain (ε_{yy}) and minor principal strain (ε_2) that are discussed at length in the manuscript. To demonstrate the typical output maps generated by the DIC technique, output from the analysis of a low aspect ratio square column (30 μm wide, 25 μm tall) is displayed in Figure S3. Vertical displacement is first evaluated at a global strain of 0.5% (Figure S3a). As local non-uniformities at the top of the column are depressed by the indenter, a vertical displacement band is formed. Note that only a small fraction of the column area is in contact with the indenter tip at initial contact, as discussed in the manuscript. This vertical displacement band expands in breadth with increasing depth into the column, further demonstrating the interconnected nature and the distributed load sharing within the array. For columns undergoing crushing, such as the column depicted in Figure S3, the initial vertical displacement band establishes a localized compressive strain slightly greater than that in the surrounding area. As a result, buckle initiation occurs in or around the vertical displacement

band established at initial contact. The establishment of a lateral buckle is observed in Figure S3(b). The buckle is established at the bottom of the vertical displacement band, and is distinguished by a large gradient in (V). Vertical displacement under the buckle is nearly zero. The vertical displacement map resolution emphasizes how the sub-pixel resolution of DIC[31] allows for nanoscale displacement and detail unattainable by SEM evaluation performed by the unassisted eye. The corresponding maps of ε_2 and ε_{yy} for this column may be found in Figure 2c.

Similarly, the horizontal displacement (U) maps for the same global strains reveal that the column is expanding slightly about its midsection while contracting slightly at the top section. The horizontal displacement increases in magnitude with global strain, introducing a horizontal (tensile) strain (Figure S3(e)). Computation of Poisson's ratio based upon this data is difficult, as the boundary conditions inhibiting the horizontal strain are uncertain for the top and bottom of the column. Regardless of the value of the Poisson's ratio, expansion about the midsection in response to compressive global strain indicates that the Poisson's ratio is a positive quantity. Finally, shear stress (Figure S3(f)) is evident near the edges of the vertical displacement band observed in Figure S3(b). The shear stress is additional evidence of the interconnected morphology of the CNT array columns and the resulting cooperative load sharing.

Supporting Videos

Video S1. High magnification i*n situ* SEM compression video of a 30 μm wide, 75 μm tall CNT array column (see Figure b).

Video S2. *In situ* SEM and DIC-generated ε_2 video obtained for a 10 μm wide, 75 μm tall CNT array column undergoing unixial compression (see Figure 3a-b).

Video S3. *In situ* SEM and DIC-generated ε_2 video obtained for a 10 μm wide, 25 μm tall CNT array column undergoing unixial compression (see Figure 3d-e).

Video S4. *In situ* SEM and DIC-generated ε_2 video obtained for a 100 μm wide, 25 μm tall CNT array column undergoing unixial compression (see Figure 4a-b).

Video S5. *In situ* SEM video obtained for a 100 μm wide,75 μm tall CNT array column undergoing unixial compression and demonstrating bottom-up buckle accumulation.

Video S6. *In situ* SEM and DIC-generated ε_2 video obtained for a 100 μm wide, 25 μm tall CNT array column undergoing unixial compression (see Figure 4d-e).

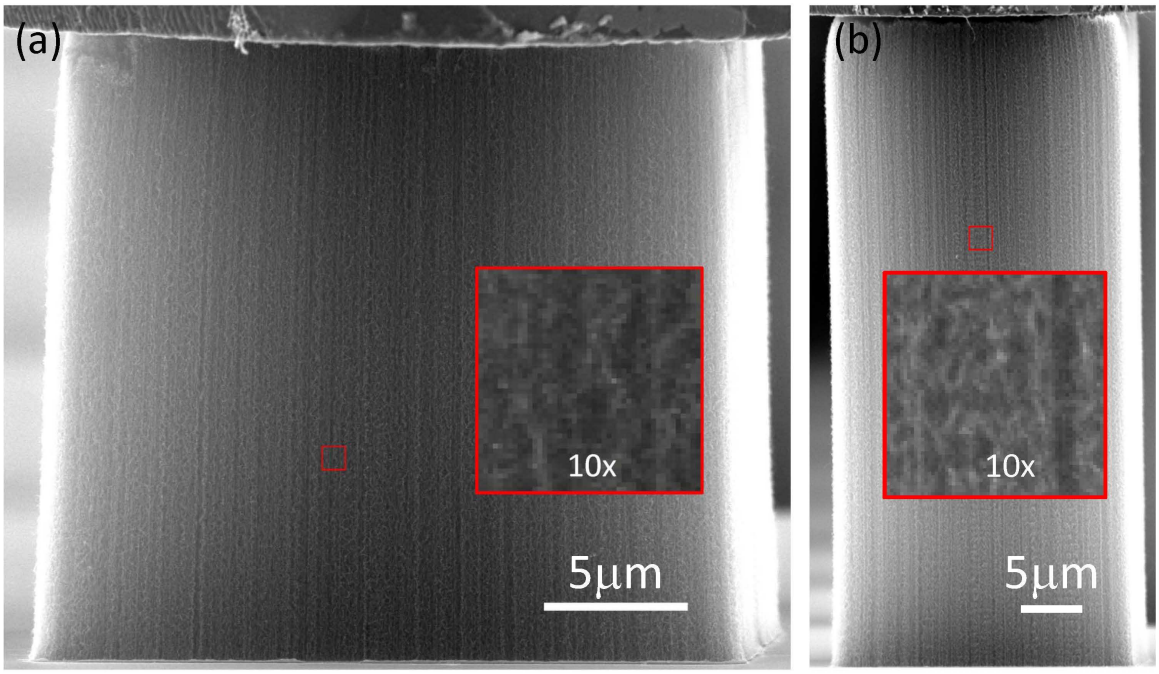

Figure S1. Typical SEM micrographs of a (a) 30 μm wide, 25 μm tall and a (b) 30 μm wide, 75 μm tall CNT array column utilized for DIC analysis. Insets show 10x enlargements of the area outlined by the small red squares and demonstrate the level of pixilation relative to the characteristic CNT diameter (8 – 10 nm) and feature sizes.

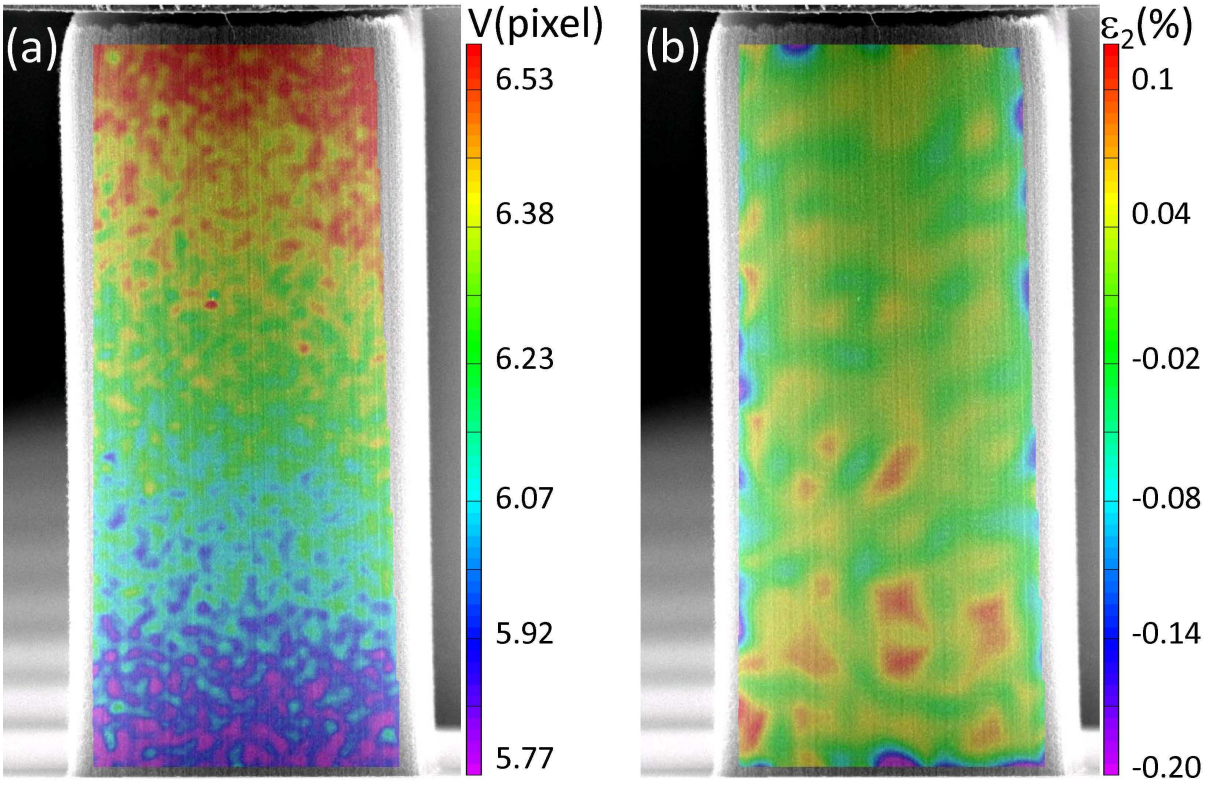

Figure S2. SEM imaging drift and scan distortion was examined utilizing a 30 μm wide, 75 μm tall CNT array column subjected to image acquisition and DIC parameters utilized for mechanical testing. After acquiring 100 images in approximately 2.5 hours, (a) translation in the vertical direction (V) due to image drift ranged between 5.77 – 6.53 pixels across the length of the column (0.76 pixel difference). (b) The corresponding minor principal strain artifact was between -0.20% – 0.1%. These error contributions are negligible with respect to the displacement and strain examined in this study.

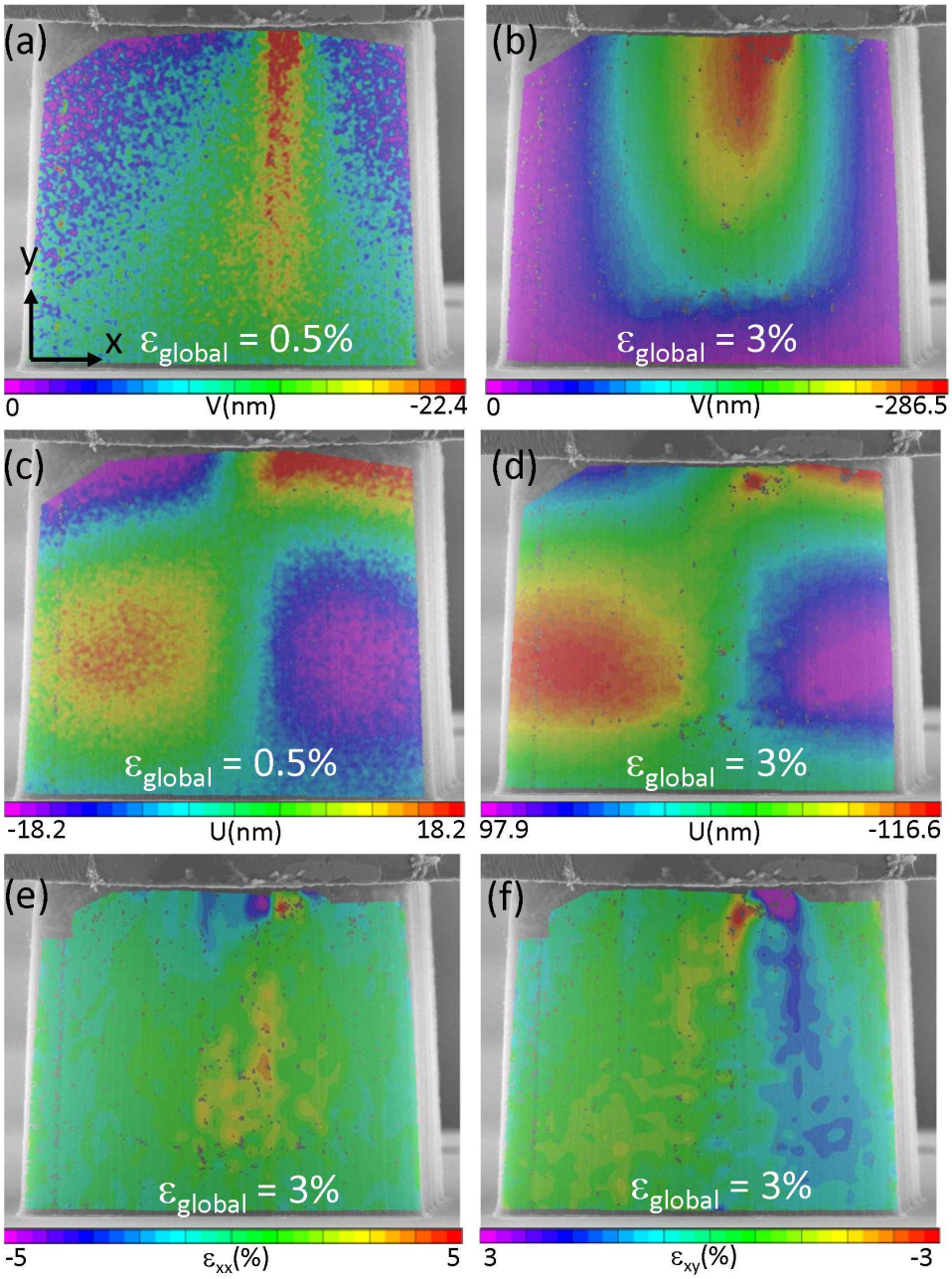

Figure S3. DIC analysis of a 30 μm wide, 25 μm tall CNT array column. Vertical displacement field (V) is evaluated at (a) 0.5% and (b) 3% global strain. Similarly, horizontal displacement (U) is evaluated at (c) 0.5% and (d) 3% global strain. (e) Lateral strain (ε_{xx}), and (f) shear stress (ε_{xy}) are evaluated at 3% global strain.